Microwave-assisted: Boron nitride nano materials based sulfonic acid catalyst for the synthesis of biologically active ethylpiperazinyl-quinolinyl fused acridine derivatives

Arul Murugesan[1], Robert M Gengan[1*], Kandasamy G Moodley[1*] and Gerhard Gericke[2]

[1]*Department of Chemistry, Faculty of Applied Sciences, Durban University of Technology, Durban 4001, South Africa*
[2]*Eskom RT&ND Laboratories, Rosherville, Gauteng, South Africa*

*Corresponding author. Tel: (+27) 31 3732309, (+27) 31 3735133; Fax: (+27)866740441, (+27)866740839;
E-mail: genganrm@dut.ac.za; moodlykg@dut.ac.za

Received: 16 November 2016, Revised: 09 December 2016 and Accepted: 20 December 2016

DOI: 10.5185/amlett.2017.1495
www.vbripress.com/aml

Abstract

Boron nitride nanomaterial based solid acid catalyst is an efficient and reusable sulfonic acid catalyst for the one-pot synthesis of 9-(2-(4-ethylpiperazin-1-yl)quinolin-3-yl)-3,3-dimethyl-3,4,9,10-tetrahydroacridin-1(2H)-one derivatives under microwave irradiation conditionsvia. The Knoevenagel and Michael type reactions. The catalyst was prepared by simply mixing boron nitride and 3-amino-4-methoxybenzenesulfonic acid in a safe method. The morphological properties of the catalyst was determined by using FT-IR, XRD, TEM, SEM and Raman spectroscopy. The synthesised catalyst was employed in a Knoevenagel and Michael type reaction to synthesise novel ethylpiperazinyl-quinolinyl based acridine derivatives. Furthermore, the newly-synthesised compounds was used for molecular docking in Hsp90 protein studies. The method developed in this study has the advantages of good yield, simplicity coupled with safety and short reaction time. Most importantly it was found that the solid acid catalyst can be recycled with minimal loss of activity over five cycles.

Keywords: Boron nitride, MW, MCRs, knoevenagel condensation.

Introduction

Multicomponent reactions (MCRs) are one-pot processes which have powerful bond-forming capability and henceutilized in combinatorial and medicinal chemistry [**1**]. One important class of compounds are benzo-acridine derivatives which have been employed as anti-bacterial [**2**], cytotoxic [**3**], anti-fungal [**4**] and anti-malarial [**5**] agents. In the last few years, acridone and acridine frameworks have become the focus of much research in producing anti-cancer drugs. Whereas they were previously targeted as antimicrobials [**6-7**], acridone and acridine moieties are being exploited in anti-melanoma reagents [**8**] and DNA binding [**9**]. These moieties have also been used in the synthesis of new acridine derivatives as polycyclics with five- or six-member ring systems. The new compounds have been studied as important DNA intercalating anticancer drugs [**10-11**]. Since cancer is considered to be the foremost cause of human death, a multitude of research groups have the goal of discovering affordable but effective anti-cancer formulations. The current treatment or therapies for cancer include surgery, radiotherapy and chemotherapy [**12-15**]. Among these therapies, chemotherapy is the most widely-used one. Unfortunately, most of the antineoplastic drugs used as therapeutic agents, have major drawbacks such as poor efficacy, increased risk of side effects and increased instances of multi-drug resistance. An additional major hurdle in cancer treatment is the non-selectivity of antineoplastic agents towards cancerous cells and normal cells [**16**]. Hence development of a potent, safe and selective antineoplastic is of prime importance to prevent cancer [**17-18**]. Benzo[*c*]acridine derivatives have been recently synthesized by a number of methods involving one-pot multi-component condensation reactions of naphthylamines, dimedone and aldehydes under various reaction conditions; for example, using triethylbenzylammonium chloride (TEBAC)/H2O [**19**], ionic liquid [**20**], under microwave irradiation (MWI) [**21-23**], or ultrasound irradiation (USI) [**24**]. Use of heterogeneous catalysts has recently received considerable interest in various organic syntheses. The SBA-15 is a nano-porous silica which has a hexagonal structure, large pore size, high surface area and good thermal constancy. It has denser aperture walls and higher aperture size. [**25**]. There are only a few reports on the applications of SBA-

Pr-SO_3H such as nano solid acid catalyst with chemical transformations [**26-29**].

Altering the surface chemistry of boron nitride (BN) is still in its early stages, and effective surface functionalization remains a challenging task. In the present study, 3-aminopropyl-triethoxysilane (APTES) was used as a silanizing agent to change the surface. APTES is an important aminosilane which has wide applications in many fields [**30**]. In particular, previous reports on multi-walled carbon nanotubes functionalized with APTES showed improved compatibility with other polymers for the application in nanotube-based polymer matrix composites [**31**]. In this study, after oxidation of BNwith concentrated nitric acid, APTES molecules were linked to the nanotube walls, thus obtaining functionalized BNNTs (f-BNNTs) with free amino groups on their surfaces. The obtained f-BNNTs were characterized through SEM (scanning electron microscopy) and TEM (transmission electron microscopy) imaging, Z-potential analysis, EDS (energy-dispersive X-ray spectroscopy) and XPS (X-ray photoelectron spectroscopy). Biocompatibility tests were performed for f-BNNTs. Thereafter the possibility of covalently binding molecules on their surface was assessed by labelling f-BNNTs with a fluorescent dye. Fluorescent f-BNNTs were finally used for in-vitro experiments, demonstrating their internalization by NIH/3T3 fibroblasts [**32**].

The more acidic ILs [DISM][CCl_3COO] and [DSIM][CF_3COO] have been efficiently utilized as recyclable catalysts for the preparation of 14*H*-dibenzo[*a*,*j*]xanthene and 1,8-dioxo-decahydroacridine derivatives in short times under solvent-free conditions at 80–100 °C with excellent yields. The above two ILs could be effectively utilized as catalysts for the synthesis of 1, 8-dioxo-decahydroacridine in water at the same temperature [**33**].

In the light of above reports, the development of novel and simple methods for the preparation of acridines containing naphthalene and quinolones fragments is much a needed research activity. In this report we describe the novel synthesis of ethylpiperazinyl-quinolinyl based acridone derivative under microwave irradiation using boron nitride nano materialas as a solid acid catalyst. The novelty of this work is due to the following aspects:

1. Synthesis of a new catalyst; Boron nitride nano material based sulfonic acid.
2. Synthesis of a new precursor; 2-(4-ethylpiperazin-1-yl) quinoline-3-carbaldehyde.
3. Synthesis of new highly functionalised novel biological active ethylpiperazinyl-quinolinyl acridine derivatives, under microwave conditions.
4. Molecular docking investigations of ethylpiperazinyl-quinolinyl acridine derivatives using Hsp90 protein.

Experimental

General

Chemicals were purchased from Merck and Sigma-Aldrich. The reaction monitoring and purity of the product was accomplished by TLC. FTIR spectra were recorded in the range of 4000-400 cm^{-1} on a JASCO FT/IR-460 spectrophotometer using KBr pellets. A Bruker D2 PHASER powder diffraction instrument; CuKα ray (wavelength λ = 0.154056 nm), was used to measure in a continuous step-scan mode: the minimum width of the stage 0.031°, equilibrium time of 256 seconds, the operating voltage to 30 kV with 10 mA. Field-emission scanning electron microscopy (FESEM, Jeol JSM 7600F) was employed to characterise the morphology. High Resolution-Transmission Electron Spectroscopy (HR-TEM) was used. The BET gas sorption isotherms were measured at 77 K for N_2 and H_2, and 273 and 298 K for CO_2 using Micromeritics Autopore 9500 system. Before recording gas sorption measurements, the sample was initially dehydrated at 423 K for 24 h under vacuum. Raman Spectroscopy was measured using the detector CCD (Triax) and the laser (He-Ne laser 632.8 nm). The NMR spectra were recorded in a Bruker Advance 400 MHz instrument. A TOF-MS analyser for accurate (HRMS) was used. The melting point (m.p) was recorded on a Buchi B-545 apparatus using open capillary tubes.

Catalyst preparation

A mixture of BN and 65% nitric acid was refluxed for 24h to activate the BN surface with OH groups.Briefly, to 10 g of BN and 15 g of 3-amino-4-methoxybenzenesulfonic acid was added 30 mL dry toluene and the reaction mixture was refluxed for 24 h. After this period, the mixture was filtered and washed with distilled water and acetone to obtain solid acid catalyst BN-PT-SO_3H (**Scheme 1**).

General Procedure for the synthesis of substituted 2-(4-ethylpiperazin-1-yl)quinoline-3-carbaldehyde (3)

In order to synthesise some new biologically potent piperazinyl-quinolinyl benzo[*c*]acridine derivatives, the starting compound 2-chloro-3-formyl quinoline (CFQ) (**1**) was prepared from acetanilide, DMF and $POCl_3$ by the Vilsmeir Haack reaction [**34**]. An aliquot (0.001 mol) of CFQ and potassium carbonate (0.002 mol) was added to a round bottom flask and an excess of 1-ethylpiperazine was added. The mixture was refluxed for 24 h at 200 °C; the reaction was monitored by TLC. After completion of the reaction, the reaction mass was cooled to room temperature and poured into water. It was then filtered, washed with water and dried. The crude product was purified by column chromatography using silica gel and a mobile phase of acetone and hexane (70:30) to produce a yellow powder of 95 % yield (m.p 220-222 °C). IR (KBr): 2979, 2934, 2643, 2901, 2358, 2333, 1693, 1615, 1593, 1421, 1372, 1239, 952, 765, 512, 482 cm^{-1}. ^{1}H NMR ($CDCl_3$, 400 MHz): δ 10.16 (1H, brs, CHO), 8.47 (1H, brs, Ar-H), 7.82 (1H, d, J = 8.4 Hz, Ar-H), 7.76-7.79 (1H, dd, J = 1 Hz, Ar-H), 7.66-7.70 (1H, m, J =1.52 Hz, Ar-H), 7.34-7.38 (1H, m, J =1.04 Hz, Ar-H), 3.53-3.55 (4H, t, J= 4.84 Hz, CH_2), 2.66-2.69 (4H, t, J=4.92 Hz, CH_2), 2.49-2.54 (2H, q, J=7.28 Hz, CH_2), 1.13-1.16 (3H, t, CH_3). ^{13}C NMR ($CDCl_3$, 100 MHz): δ 190.27, 159, 149.35, 142.18, 132.41, 129.24, 127.56, 124.55, 123.98, 122.06, 52.70, 52.38, 51.04, 11.97. TOF

MS ES+ Calc. mass 270.16, Found: 270.15 Anal. Calc. For $C_{16}H_{19}N_3O$: C, 71.35; H, 7.11; N, 15.60 %. Found: C, 71.37; H, 7.12; N, 15.62 %. This compound was fully characterised by IR, ^{1}H-NMR, ^{13}C-NMR, TOF-MS and elemental analysis (**Fig. 7-8** in Supporting information).

General Procedure for the synthesis of 9-(2-(4-ethylpiperazin-1-yl)quinolin-3-yl)-3,3-dimethyl-3,4,9,10-tetrahydroacridin-1(2H)-one (6a-p)

The sulfonic acid functionalized BN-PT-SO_3H solid acid catalyst (0.07g) was activated in vacuum at 100 °C and then after cooling to room temperature, 2-(4-ethylpiperazin-1-yl) quinoline-3-carbaldehyde (1.0 mmol), dimidone (1.0 mmol), and aniline (1.0 mmol) were added to it. The mixture was heated at 140 °C in MW, conditions at 120W for an appropriate time as shown in **Table 2**. The reaction was monitored by TLC. After the completion of the reaction, the mixture was dissolved in ethanol in order to separate catalyst and then the filtrate was cooled to afford the purified Colum chromatography acetone and hexane pure product. The catalyst was washed subsequently with diluted acid solution, distilled water and then acetone, dried under vacuum and recycled for several times without loss of significant activity. The spectral (^{1}H NMR, ^{13}C NMR, MS, elemental analysis and IR) data for new compounds are given below. And compound **6a** (see **Fig. 9-10** in supporting information).

Spectroscopic information

9-(2-(4-ethylpiperazin-1-yl)quinolin-3-yl)-3,3-dimethyl-3,4,9,10-tetrahydroacridin-1(2H)-one (6a)

White colour solid: IR (KBr): 3495, 3236, 3159, 2961, 2259, 1681, 1630, 1568, 1434, 1358, 1196, 1135, 999, 764, 571 cm^{-1}. ^{1}H NMR ($CDCl_3$, 400 MHz): δ 12.98 (1H, s, N-H), 8.10 (1H, s, Ar-H), 7.65 (2H, d, J = 7.6 Hz, Ar-H), 7.43-7.45 (2H, t, J = 7.2 Hz, Ar-H), 7.20-730 (2H, t, J = 12 Hz, Ar-H), 7.17 (2H, d, J = 7.6 Hz, Ar-H), 4.82 (1H, s, CH), 2.47 (6H, m, CH_2), 2.12-2.25 (8H, q, CH_2), 1.05 (6H, s, CH_3), 0.88 (3H, s, CH_3). ^{13}C NMR ($CDCl_3$, 100 MHz): δ197.17, 164.77, 163.32, 141.10, 138.20, 130.32, 129.41, 129.25, 129.05, 128.98, 128.52, 122.11, 120.32, 119.70, 115.01, 111.58, 52.88, 52.04, 50.88, 41, 32.18, 32, 31.16, 30.92, 29.32, 26.95. TOFMS ES *m/z* (rel. int.): 457.12 [M]$^+$. Anal. Calc. for $C_{30}H_{34}N_4O$: C, 77.22; H, 7.34; N, 12.01 %. Found: C, 77.24; H, 7.36; N, 12.12 %.

9-(2-(4-ethylpiperazin-1-yl)quinolin-3-yl)-3,3-dimethyl-5-nitro-3,4,9,10-tetrahydroacridin-1(2H)-one (6b)

White colour solid: IR (KBr): 3319, 3164, 3106, 3066, 2963, 2306, 1968, 1812, 1680, 1636, 1568, 1480, 1487, 1194, 1136, 999, 929, 764 cm^{-1}. ^{1}H NMR ($CDCl_3$, 400 MHz): δ 11.84 (1H, s, N-H), 8.01 (1H, s, Ar-H), 7.76 (1H, d, J = 8.4 Hz, Ar-H), 7.57 (2H, d, J = 7.6 Hz, Ar-H), 7.34-7.38 (3H, t, J = 7.8 Hz, Ar-H), 4.73 (1H, s, CH), 3.49-3.88 (4H, m, CH_2), 2.39 (4H, m, CH_2), 2.05-2.17 (6H, q, CH_2), 1.18 (3H, s, CH_3), 0.99 (3H, s, CH_3), 0.84 (3H, s, CH_3). ^{13}C NMR ($CDCl_3$, 100 MHz): δ 197.16, 164.74, 162.81, 141.15, 137.96, 130.88, 130.44, 129.52, 128.80, 128.57, 127.65, 122.22, 120.32, 114.82, 50.89, 49.79, 40.97, 38.73, 32.18, 31.11, 29.69, 29.32, 28.92, 27.02, 22.98. Anal. Calc. for $C_{30}H_{33}N_5O_3$: C, 70.43; H, 6.50; N, 13.69 %. Found: C, 70.42; H, 6.52; N, 13.67 %.

9-(2-(4-ethylpiperazin-1-yl)quinolin-3-yl)-3,3-dimethyl-7-nitro-3,4,9,10-tetrahydroacridin-1(2H)-one (6c)

White colour solid: IR (KBr): 3496, 3236, 3159, 2961, 2259, 1968, 1811, 1681, 1630, 1568, 1434, 1358, 1196, 1135, 999, 929, 764, 571 cm^{-1}. ^{1}H NMR ($CDCl_3$, 400 MHz): δ 12.99 (1H, s, N-H), 8.12 (1H, s, Ar-H), 7.66 (2H, d, J = 7.6 Hz, Ar-H), 7.44-7.49 (2H, dd, J = 6.8 Hz, Ar-H), 7.32(2H, d, J = 8.4 Hz, Ar-H), 7.18 (1H, s, Ar-H), 4.82 (1H, s, CH), 2.47 (6H, m, CH_2), 2.13-2.25 (8H, q, CH_2), 1.06 (6H, s, CH_3), 0.89 (3H, s, CH_3). ^{13}C NMR ($CDCl_3$, 100 MHz): δ 197.16, 164.79, 163.26, 141.25, 138.14, 130.19, 129.46, 128.58, 122.18, 120.38, 115.82, 111.54, 50.89, 41.01, 32.19, 31.21, 29.32, 26.98. Anal. Calc. for $C_{30}H_{33}N_5O_3$: C, 70.43; H, 6.50; N, 13.69 %. Found: C, 70.44; H, 6.53; N, 13.67 %.

9-(2-(4-ethylpiperazin-1-yl)quinolin-3-yl)-7-fluoro-3,3-dimethyl-3,4,9,10-tetrahydroacridin-1(2H)-one (6d)

White colour solid: IR (KBr): 3456, 3307, 3159, 3108, 3060, 2961, 2915, 2361, 1966, 1811, 1664, 1663, 1589, 1466, 1434, 1366, 1197, 1165, 1136, 999, 765, 571 cm^{-1}. ^{1}H NMR ($CDCl_3$, 400 MHz): δ 12.87 (1H, s, N-H), 8.11 (1H, s, Ar-H), 7.66 (2H, d, J = 8 Hz, Ar-H), 7.44-7.48 (2H, t, J = 7.6 Hz, Ar-H), 7.32(2H, d, J = 8.4 Hz, Ar-H), 7.17 (1H, s, Ar-H), 4.82 (1H, s, CH), 2.47 (6H, m, CH_2), 2.13-2.21 (8H, t, CH_2), 1.06 (6H, s, CH_3), 0.89 (3H, s, CH_3). ^{13}C NMR ($CDCl_3$, 100 MHz): δ 197.18, 164.77, 163.22, 141.14, 138.17, 130.30, 129.43, 128.56, 122.14, 120.34, 114.97, 111.58, 50.89, 41.01, 32.19, 32.01, 31.18, 29.32, 26.98. ^{19}F NMR ($CDCl_3$, 400 MHz): δ -120.68, -115.81, -113.31. Anal. Calc. for $C_{30}H_{33}FN_4O$: C, 74.35; H, 6.86; N, 11.56 %. Found: C, 74.37; H, 6.87; N, 11.58 %.

7-chloro-9-(2-(4-ethylpiperazin-1-yl)quinolin-3-yl)-3,3-dimethyl-3,4,9,10-tetrahydroacridin-1(2H)-one (6e)

White colour solid: IR (KBr): 3474, 3306, 3161, 3108, 3062, 2961, 2918, 2367, 1969, 1811, 1661, 1568, 1434, 1359, 1197, 1165, 1135, 765, 572 cm^{-1}. ^{1}H NMR ($CDCl_3$, 400 MHz): δ 12.31 (1H, s, N-H), 8.16 (1H, s, Ar-H), 7.68 (3H, d, J = 8 Hz, Ar-H), 7.56 (1H, d, J = 7.6 Hz, Ar-H), 7.31-7.48 (3H, t, J = 7.6 Hz, Ar-H), 7.29 (1H, s, Ar-H), 4.83 (1H, s, CH), 2.48 (6H, m, CH_2), 2.14-2.26 (8H, q, CH_2), 1.07 (6H, s, CH_3), 0.93 (3H, s, CH_3). ^{13}C NMR ($CDCl_3$, 100 MHz): δ 197.17, 164.83, 162.68, 141.91, 137.64, 129.85, 128.68, 122.66, 120.57, 115.11, 111.41, 50.88, 40.97, 32.19, 32.20, 29.29, 27.07. Anal. Calc. for $C_{30}H_{33}ClN_4O$: C, 71.91; H, 6.64; N, 11.18 %. Found: C, 71.89; H, 6.66; N, 11.16 %.

7,8-dichloro-9-(2-(4-ethylpiperazin-1-yl)quinolin-3-yl)-3,3-dimethyl-3,4,9,10-tetrahydroacridin-1(2H)-one (6f)

White colour solid: IR (KBr): 3308, 3105, 3161, 3067, 2961, 2915, 2364, 2327, 1969, 1812, 1667, 1664, 1568, 1434, 1408, 1360, 1197, 1135, 999, 765, 571, 514 cm^{-1}. ^1H NMR ($CDCl_3$, 400 MHz): δ 12.16 (1H, s, N-H), 8.12 (1H, s, Ar-H), 7.64 (2H, d, J = 8 Hz, Ar-H), 7.47 (1H, d, J = 7.6 Hz, Ar-H), 7.45 (2H, d, J = 7.8 Hz, Ar-H), 7.19 (1H, d, J = 7.4 Hz, Ar-H), 4.83 (1H, s, CH), 3.76-3.90 (2H, t, CH_2), 2.48 (4H, m, CH_2), 2.14-2.26 (6H, q, CH_2), 1.07 (6H, s, CH_3), 0.92 (3H, s, CH_3). ^{13}C NMR ($CDCl_3$, 100 MHz): δ 197.17, 164.78, 162.72, 141.41, 137.83, 130.27, 129.65, 128.61, 122.40, 120.43, 114.92, 111.55, 50.89, 40.97, 32.19, 31.11, 30.93, 29.30, 27.05. Anal. Calc. for $C_{30}H_{32}Cl_2N_4O$: C, 67.29; H, 6.02; N, 10.46 %. Found: C, 67.32; H, 6.05; N, 10.45 %.

7-bromo-9-(2-(4-ethylpiperazin-1-yl)quinolin-3-yl)-3,3-dimethyl-3,4,9,10-tetrahydroacridin-1(2H)-one (6g)

White colour solid: IR (KBr): 3308, 3162, 3108, 3037, 2961, 2306, 1968, 1812, 1625, 1568, 1487, 1437, 1434, 1408, 1356, 1198, 1136, 999, 764, 571 cm^{-1}. ^1H NMR ($CDCl_3$, 400 MHz): δ 12.42 (1H, s, N-H), 8.14 (1H, s, Ar-H), 7.64 (2H, d, J = 8 Hz, Ar-H), 7.49 (1H, s, Ar-H), 7.31-7.47 (2H, t, J = 7.2 Hz, Ar-H), 7.28 (2H, d, J = 7.8 Hz, Ar-H), 4.83 (1H, s, CH), 2.48 (6H, m, CH_2), 2.14-2.26 (8H, q, CH_2), 1.07 (6H, s, CH_3), 0.92 (3H, s, CH_3). ^{13}C NMR ($CDCl_3$, 100 MHz): δ 197.17, 164.80, 162.88, 141.54, 137.87, 130.06, 129.64, 128.64, 122.41, 120.47, 115.01, 111.48, 50.89, 40.99, 32.19, 31.20, 29.30, 27.03. Anal. Calc. for $C_{30}H_{33}BrN_4O$: C, 66.05; H, 6.10; N, 10.27 %. Found: C, 66.08; H, 6.13; N, 10.28 %.

9-(2-(4-ethylpiperazin-1-yl)quinolin-3-yl)-3,3,5-trimethyl-3,4,9,10-tetrahydroacridin-1(2H)-one (6h)

White colour solid: IR (KBr): 3474, 3309, 3159, 3111, 3066, 2962, 2376, 1972, 1812, 1664, 1626, 1565, 1434, 1360, 1197, 1165, 1135, 999, 929, 765, 571, 467 cm^{-1}. ^1H NMR ($CDCl_3$, 400 MHz): δ 12.69 (1H, s, N-H), 8.13 (1H, s, Ar-H), 7.67 (1H, d, J = 7.6 Hz, Ar-H), 7.47-7.49 (3H, t, J = 7.4 Hz, Ar-H), 7.45(1H, d, J = 1.2 Hz, Ar-H), 7.32 (2H, t, J = 8.2 Hz, Ar-H), 4.82 (1H, s, CH), 2.47 (6H, m, CH_2), 2.13-2.26 (8H, q, CH_2), 1.06 (6H, s, CH_3), 0.96 (6H, s, CH_3). ^{13}C NMR ($CDCl_3$, 100 MHz): δ 197.17, 164.80, 163.06, 141.43, 137.98, 130.11, 129.57, 128.62, 122.33, 120.44, 115.02, 111.50, 50.89, 40.99, 32.19, 31.21, 29.31, 27.01. Anal. Calc. for $C_{31}H_{36}N_4O$: C, 77.47; H, 7.55; N, 11.66%. Found: C, 77.49; H, 7.57; N, 11.68%.

9-(2-(4-ethylpiperazin-1-yl)quinolin-3-yl)-3,3,6-trimethyl-3,4,9,10-tetrahydroacridin-1(2H)-one (6i).

White colour solid: IR (KBr): 3507, 3306, 3160, 2961, 2315, 1969, 1812, 1668, 1646, 1568, 1434, 1197, 1135, 999, 929, 764, 571 cm^{-1}. ^1H NMR ($CDCl_3$, 400 MHz): δ 12.69 (1H, s, N-H), 8.13 (1H, s, Ar-H), 7.67 (2H, d, J = 7.6 Hz, Ar-H), 7.45-7.49 (2H, dd, J = 7.2 Hz, Ar-H), 7.32 (2H, d, J = 8.4 Hz, Ar-H), 7.18 (1H, s, Ar-H), 4.83 (1H, s, CH), 2.47 (6H, m, CH_2), 2.13-2.26 (8H, q, CH_2), 1.06 (6H, s, CH_3), 0.96 (6H, s, CH_3). ^{13}C NMR ($CDCl_3$, 100 MHz): δ 197.17, 164.80, 163.09, 141.42, 138.01, 130.11, 129.56, 128.62, 122.30, 120.43, 115.02, 111.51, 50.89, 41, 32.19, 31.21, 29.31, 27.01. Anal. Calc. for $C_{31}H_{36}N_4O$: C, 77.47; H, 7.55; N, 11.66 %. Found: C, 77.45; H, 7.57; N, 11.64 %.

9-(2-(4-ethylpiperazin-1-yl)quinolin-3-yl)-3,3,7-trimethyl-3,4,9,10-tetrahydroacridin-1(2H)-one (6j)

White colour solid: IR (KBr): 3307, 3158, 3114, 3066, 2961, 2918, 2860, 2367, 1963, 1939, 1812, 1664, 1568, 1434, 1360, 1197, 1135, 1166, 999, 764, 571 cm^{-1}. ^1H NMR ($CDCl_3$, 400 MHz): δ 12.74 (1H, s, N-H), 8.13 (1H, s, Ar-H), 7.67 (2H, d, J = 7.8 Hz, Ar-H), 7.45-7.49 (2H, dd, J = 7.4 Hz, Ar-H), 7.32 (2H, d, J = 8.2 Hz, Ar-H), 7.18 (1H, s, Ar-H), 4.82 (1H, s, CH), 2.47 (6H, m, CH_2), 2.13-2.26 (8H, q, CH_2), 1.06 (6H, s, CH_3), 0.90 (6H, s, CH_3). ^{13}C NMR ($CDCl_3$, 100 MHz): δ 197.17, 164.79, 163.15, 141.35, 138.06, 130.14, 129.52, 128.61, 122.26, 120.41, 115.01, 111.52, 50.89, 41, 32.19, 31.19, 31.21, 29.31, 27. Anal. Calc. for $C_{31}H_{36}N_4O$: C, 77.47; H, 7.55; N, 11.66 %. Found: C, 77.48; H, 7.57; N, 11.67 %.

9-(2-(4-ethylpiperazin-1-yl)quinolin-3-yl)-3,3,5,7-tetramethyl-3,4,9,10-tetrahydroacridin-1(2H)-one (6k)

White colour solid: IR (KBr): 3615, 3304, 3158, 3111, 3063, 2962, 2367, 1968, 1812, 1638, 1568, 1434, 1360, 1197, 1135, 999, 764, 572, 514 cm^{-1}. ^1H NMR ($CDCl_3$, 400 MHz): δ 12.72 (1H, s, N-H), 8.11 (1H, s, Ar-H), 7.65-7.67 (1H, t, J = 0.8 Hz, Ar-H), 7.46-7.48 (2H, t, J = 7.2 Hz, Ar-H), 7.44 (1H, d, J = 0.8 Hz, Ar-H),7.32 (2H, d, J = 8 Hz, Ar-H), 4.82 (1H, s, CH), 3.90 (2H, d, CH_2), 2.47 (4H, m, CH_2), 2.13-2.25 (8H, q, CH_2), 1.06 (6H, s, CH_3), 0.89 (9H, s, CH_3). ^{13}C NMR ($CDCl_3$, 100 MHz): δ 197.17, 164.76, 163.15, 141.16, 138.15, 130.28, 129.43, 128.57, 122.14, 120.34, 114.94, 111.56, 50.89, 41, 32.19, 31.20, 29.31, 26.99. Anal. Calc. for $C_{32}H_{38}N_4O$: C, 77.70; H, 7.74; N, 11.33%. Found: C, 77.72; H, 7.76; N, 11.36%.

9-(2-(4-ethylpiperazin-1-yl)quinolin-3-yl)-5-methoxy-3,3-dimethyl-3,4,9,10-tetrahydroacridin-1(2H)-one (6l)

White colour solid: IR (KBr): 3307, 3159, 3111, 3063, 2960, 2315, 1969, 1812, 1664, 1663, 1568, 1434, 1197, 1136, 765, 572, 514 cm^{-1}. ^1H NMR ($CDCl_3$, 400 MHz): δ 12.68 (1H, s, N-H), 8.13 (1H, s, Ar-H), 7.67 (1H, d, J = 7.6 Hz, Ar-H), 7.47-7.49 (2H, dd, J = 7.4 Hz, Ar-H), 7.32 (1H, d, J = 8 Hz, Ar-H), 7.19-7.23 (3H, t, J = 7.2 Hz, Ar-H), 4.83 (1H, s, CH), 2.47 (6H, m, CH_2), 2.13-2.26 (8H, q, CH_2), 1.05 (6H, s, CH_3), 0.91 (6H, s, CH_3). ^{13}C NMR ($CDCl_3$, 100 MHz): δ 197.16, 164.74, 162.81, 141.15, 137.96, 130.88, 130.44, 129.52, 128.80, 128.57, 127.65, 122.22, 120.32, 114.82, 68.16, 50.89, 49.79, 40.97, 38.73, 32.18, 31.11, 29.69, 29.32, 28.92, 27.02, 22.98. Anal. Calc. for $C_{31}H_{36}N_4O_2$: C, 74.97; H, 7.31; N, 11.28%. Found: C, 74.95; H, 7.33; N, 11.27%.

9-(2-(4-ethylpiperazin-1-yl)quinolin-3-yl)-7-methoxy-3,3-dimethyl-3,4,9,10-tetrahydroacridin-1(2H)-one (6m)

White colour solid: IR (KBr): 3319, 3165, 3102, 3069, 2963, 2364, 1968, 1811, 1677, 1664, 1627, 1568, 1498, 1434, 1362, 1200, 1136, 999, 929, 765, 572, 514 cm^{-1}. ^1H NMR ($CDCl_3$, 400 MHz): δ 11.73 (1H, s, N-H), 8.11 (1H, s, Ar-H), 7.62 (2H, d, J = 7.6 Hz, Ar-H), 7.43-7.47 (1H, t, J = 7.2 Hz, Ar-H), 7.25 (2H, t, J = 16.4 Hz, Ar-H), 7.19 (2H, d, J = 7.8 Hz, Ar-H), 4.82 (1H, s, CH), 3.72-3.94 (2H, m, CH_2), 2.48 (4H, m, CH_2), 2.14-2.26 (6H, q, CH_2), 1.73 (2H, s, CH_2), 1.09 (6H, s, CH_3), 0.91 (6H, s, CH_3).^{13}C NMR ($CDCl_3$, 100 MHz): δ 197.16, 164.74, 162.81, 141.15, 137.96, 130.88, 130.44, 129.52, 128.80, 128.57, 127.65, 122.22, 120.32, 114.82, 68.16, 50.89, 49.79, 40.97, 38.73, 32.18, 31.11, 29.69, 29.32, 28.92, 27.02, 22.98. Anal. Calc. for $C_{31}H_{36}N_4O_2$: C, 74.97; H, 7.31; N, 11.28 %. Found: C, 74.96; H, 7.33; N, 11.30 %.

5-(2-(4-ethylpiperazin-1-yl)quinolin-3-yl)-8,8-dimethyl-5,8,9,10-tetrahydrobenzo[b][1,8]naphthyridin-6(7H)-one (6n)

White colour solid: IR (KBr): 3309, 3157, 3114, 3063, 2962, 2312, 1968, 1811, 1677, 1640, 1568, 1487, 1434, 1368, 1134, 962, 764, 522, 514 cm^{-1}. ^1H NMR ($CDCl_3$, 400 MHz): δ 12.24 (1H, s, N-H), 8.15 (1H, s, Ar-H), 7.68 (2H, d, J = 7.6 Hz, Ar-H), 7.46-7.49 (2H, t, J = 7.2 Hz, Ar-H), 7.24-7.30 (3H, t, J = 7.84 Hz, Ar-H), 4.83 (1H, s, CH), 2.48 (6H, m, CH_2), 2.07-2.26 (8H, m, CH_2), 1.07 (6H, s, CH_3), 0.93 (3H, s, CH_3). ^{13}C NMR ($CDCl_3$, 100 MHz): δ 197.17, 164.76, 163.15, 141.16, 138.15, 130.28, 129.43, 128.57, 122.14, 120.34, 114.94, 111.56, 50.89, 41, 32.19, 31.20, 29.31, 26.99. Anal. Calc. for $C_{29}H_{33}N_5O$: C, 74.49; H, 7.11; N, 14.98 %. Found: C, 74.50; H, 7.13; N, 15 %.

5-(2-(4-ethylpiperazin-1-yl)quinolin-3-yl)-4,8,8-trimethyl-5,8,9,10-tetrahydrobenzo[b][1,8]naphthyridin-6(7H)-one (6o)

White colour solid: IR (KBr): 3481, 3319, 3160, 3066, 1664, 1360, 1568, 1434, 1197, 1135, 1165, 999, 764, 571, 514 cm^{-1}. ^1H NMR ($CDCl_3$, 400 MHz): ^1H NMR ($CDCl_3$, 400 MHz): δ 12.70 (1H, s, N-H), 8.13 (1H, s, Ar-H), 7.67 (2H, d, J = 7.6 Hz, Ar-H), 7.45-7.49 (1H, dd, J = 7.2 Hz, Ar-H), 7.32(2H, d, J = 7.86 Hz, Ar-H), 7.15 (1H, t, J = 12.6 Hz, Ar-H), 4.82 (1H, s, CH), 2.47 (6H, m, CH_2), 2.13-2.26 (8H, q, CH_2), 1.07 (6H, s, CH_3), 0.90 (6H, s, CH_3). ^{13}C NMR ($CDCl_3$, 100 MHz): δ 197.17, 164.79, 163.06, 141.42, 137.99, 130.11, 129.56, 128.62, 122.31, 120.43, 115.02, 111.50, 50.89, 41, 32.19, 31.21, 29.31, 27.01. Anal. Calc. for $C_{30}H_{35}N_5O$: C, 74.81; H, 7.32; N, 14.54 %. Found C, 74.83; H, 7.35; N, 14.56 %.

7-(2-(4-ethylpiperazin-1-yl)quinolin-3-yl)-10,10-dimethyl-7,10,11,12-tetrahydrobenzo[c]acridin-8(9H)-one (6p)

White colour solid: IR (KBr): 3306, 3163, 3108, 2961, 2921, 2358, 2336, 2297, 1811, 1667, 1664, 1625, 1568, 1487, 1434, 1360, 1197, 1135, 1165, 764 cm^{-1}. ^1H NMR ($CDCl_3$, 400 MHz): δ 12.72 (1H, s, N-H), 8.11 (1H, s, Ar-H), 7.65-7.67 (2H, t, J = 7.68 Hz, Ar-H), 7.44-7.48 (4H, dd, J = 8.4 Hz, Ar-H), 7.31 (2H, d, J = 7.4 Hz, Ar-H), 7.18 (2H, d, J = 6.8 Hz, Ar-H), 7.17 (2H, d, J = 7.6 Hz, Ar-H), 4.82 (1H, s, CH), 2.47 (6H, m, CH_2), 2.13-2.25 (8H, q, CH_2), 1.06 (6H, s, CH_3), 0.89 (3H, s, CH_3). ^{13}C NMR ($CDCl_3$, 100 MHz): δ 197.16, 164.74, 162.81, 141.15, 137.96, 130.88, 130.44, 129.52, 128.80, 128.57, 127.65, 122.22, 120.32, 114.82, 50.89, 49.79, 40.97, 38.73, 32.18, 31.11, 29.69, 29.32, 28.92, 27.02, 22.98. Anal. Calc. for $C_{34}H_{36}N_4O$: C, 79.04; H, 7.02; N, 10.84 %. Found: C, 79.06; H, 7.04; N, 10.86 %.

Molecular docking studies

Molecular docking and pharmacophore model are the two potent methods in drug discovery process. Virtual screening followed by docking has become one of the reputable methods for drug discovery and enhancing the efficiency in optimization. The main advantage of pharmacophore-based docking was to focus on specific key interaction for protein–ligand binding. To improve the selection of active compounds, it is optimal to use both methods, namely, molecular docking and pharmacophore [**35**]. Molecular docking was executed for accurate docking of ligands into protein active sites using Ligand Fit module in DS. There are three stages in Ligand Fit protocol: (i) Docking: attempt is made to dock a ligand into a user defined binding site (ii) In-Situ Ligand Minimization and (iii) Scoring: various scoring functions are calculated for each position of the ligands.

The protein complexes were selected from a protein databank (PDB, www.rcsb.org). To date, many Hsp90 complexes have been reported. From them PDB ID: 3EKO was selected, based on the resolution of the complex and the size of the co-crystal. For docking study, the protein was prepared by removing all water compounds. Force field was applied using Receptor–Ligand Interactions tool in DS. After the protein preparation, the active site of the protein has to be identified. The active site of the protein is represented as the binding site; it is a set of points on a grid that lies in a cavity. Two methods were applied to define the binding site for a protein: (i) Firstly, binding sites were identified based on the shape of the receptor using "eraser" algorithm and (ii) Secondly, by the volume occupied by the known ligand already in an active site.

In this study, binding site was defined using second method and the critical amino acids were identified by analysing the protein–ligand interactions from 40 Hsp90 co-crystal structures which were deposited in PDB. All the ligands in the complex structures showed hydrogen bond interactions with ASP93, LYS58 and hydrophobic interactions with ASN51, ALA55, GLU58, GLN97, MET98 and SER-99. This clearly indicates that the two-hydrogen bonded amino acids play a crucial role in Hsp90 inhibitors.

Results and discussion

In the present study, we report a one-pot multicomponent synthesis of highly functionalised ethylpiperazinyl-quinolinyl alcidine derivatives under microwave

conditions using nanocrystalline boron nitride-based sulfonic acid catalyst. The catalyst was synthesised in 2 stages: a mixture of BN and 65% nitric acid was refluxed for 24h. This preliminary step was to introduce –OH groups on the surface of BN through an oxidation process .After that BN and 3-amino-4-methoxybenzenesulfonic acid were refluxed for 24 h and after the work-up of the reaction, the product was formed. The mixture was filtered and washed with distilled water and acetone to obtain solid acid catalyst (**Scheme 1**). The catalyst was characterised completely by several techniques.

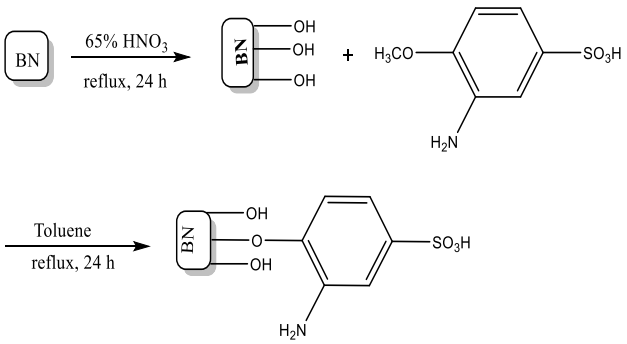

Scheme 1. The reaction scheme for the synthesis of BN-PT-SO_3H.

The FT-IR spectra for pure BN and BN-PT-SO_3H revealed the following information: in the case of BN, the absorption at 958, 1414, 2351 and 1645 cm^{-1} corresponds to the -OH stretching and bending vibrations of the adsorbed water. The spectrum of BN-PT-SO_3H is similar to BN however the absorption at 3243 cm^{-1} is flattened which can be attributed to the modification of BN. Also, the CH stretching vibrations of silylating agent was observed at 2954 cm^{-1} and the absorption at 1211 cm^{-1} is due to the C=C stretching vibration. Furthermore, the absorptions at 1163 and 1141 cm^{-1} is due to the stretching mode of S=O in SO_3H.

The XRD patterns of BN and BN-PT-SO_3H (see **Fig. S 1** in supporting information**)** clearly show the lines for anatase. It seems that the peak intensities of BN-PT-SO_3H are almost the same as those of BN thereby suggesting that the sulphate modification does not change the phase of BN.

The representative SEM images of BN (see **Fig. S2** in supporting information**)** exhibit an aggregation of cloud-like structures of small spherical-shaped particles. The SEM micrographs of BN-PT-SO_3H show some modifications with respect to BN such that the primary surface structure of BN has changed, however the cloud-like structure and small spherical-shaped particles still exists. The EDS analysis for BN and BN-PT-SO_3H (see **Fig. S3** in supporting information**)** confirms the presence of all the elements and the actual weight % is presented in BN Element B, N, O, C, S, weight % 31.60, 41.75, 1.69, 0, 0, Atomic (%) 52.95, 44.14, 1.56, 0, 0, The catalyst BN-PT-SO_3H Element B, N, O, C, S, weight % 41.56, 49.10, 1.28, 4.56, 0.08, Atomic (%) 49.10, 44.77, 1.02, 4.58, 0.03, respectively.

Field-emission scanning electron microscopy was employed to characterise the morphology. TEM image for different orientations was done to get the average crystallite size of, BN-PT-SO_3H. TEM images of BN and BN-PT-SO_3H are shown in (see **Fig. S 4** in supporting information**)** snapped at different orientations of BN (a-1um, b-200, and c-500nm) BN-Pr-SO_3H (d-1um, e-100, and f-500nm); the figure shows the crystalline size of BN-PT-SO_3H which also shows a BN-PT-SO_3H (1um for catalyst good mesoporous structures thereby suggesting a good surface for catalytic activity).

The term hydrophobic literally means water-fearing and it describes the segregation of water and nonpolar substances. Further, extensive hydrogen bonding between molecules of water reduces the area available for interaction between water and nonpolar molecules.

At higher temperatures, when water molecules become more mobile, this energy gain decreases the length of hydrogen bonds. For isomorphous specimens where no periodicities are present a numerical method for lattice fringe space measurements in HRTEM has to be used so that bright and dark field systems can be shown up

The porous properties of BN and BN-PT-SO_3H, analysed (see **Fig. S 5** in supporting information**)** by N_2 gas sorption measurements at 273K, showed BN as a type-I adsorption isotherm which is characteristic of microporous material and the BET and Langmuir surface area of BN were calculated as 18 and 46 m^2/g, respectively. The N_2 adsorption isotherm of BN-PT-SO_3H also indicated a type-I adsorption isotherm however the BET and Langmuir surface area were calculated as 6 and 9 m^2/g, respectively.

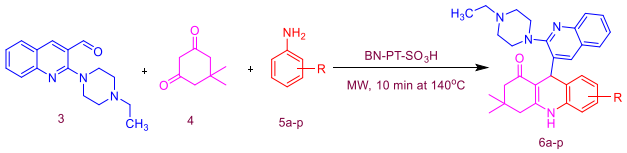

Scheme 2. The synthesis of 9-(2-(4-ethylpiperazin-1-yl) quinolin-3-yl)-3, 3-dimethyl-3, 4, 9, 10-tetrahydroacridin-1(2H)-one derivatives.

Table 1. Optimization of the synthesis of **6a** under MW irradiation system using BN-PT-SO_3H.

Entry	Catalyst	Solvent	Temp (℃)	Time (h)	Yield (%)
1	BN- PT-SO_3H	EtOH	r.t	24	60
2	BN- PT-SO_3H	MeOH	r.t	24	50
3	BN- PT-SO_3H	CH_3CN	110	24	80
4	BN- PT-SO_3H	EtOH	100	24	65
5	BN- PT-SO_3H	MeOH	100	24	58
6	BN- PT-SO_3H	Neat	140	10(min)	97

Further investigation of the structure of BN and BN-PT-SO_3H were investigated by Raman spectroscopy (see **Fig. S 6** in supporting information**)** which showed absorption signals at 600, 1480, 2000, 3000, and 3750 cm^{-1} for BN. The absorption signal of BN-PT-SO_3H showed absorptions signals at 600, 2000, 3000, 3750 cm^{-1} with an additional signal at 3250 cm^{-1} indicating the acidic functional group.

In order to synthesise some new biologically potent ethylpiperazinyl-quinolinyl acridine derivatives, a new starting compound viz., 2-(4-ethylpiperazin-1-yl) quinoline-3-carbaldehyde (**3**) was synthesised after using the Vilsmeir-Haack reaction to prepare 2-chloroquinoline-3-carbaldehyde (**1**) from acetanilide [**34**]. Thereafter a mixture of **1** and 1-ethylpiperazine (**2**) was refluxed in a basic medium to obtain **3** after 24 hours. This compound was fully characterised by IR, ^{1}H-NMR, ^{13}C-NMR, TOF-MS and elemental analysis (**Fig. S 7-8** in Supporting information).

In a preliminary study to synthesise **6a** (**Scheme 2**) we compared a solvent-free system against ethanol and observed better yield in the latter case. Hence to determine the optimum quantity of BN-PT-SO_3H, the condensation of **3**, dimidone (**4**) and aniline (**5a**), (**Scheme 2**) was carried out in the presence of different amount of catalyst (0.02, 0.05, 0.07 g) under MW conditions: **6a** was produced and subsequently characterised by IR, ^{1}H-NMR, ^{13}C-NMR, TOF-MS and elemental analysis. It was found that increasing the quantity of the catalyst beyond 0.05 g did not increase the yield noticeably hence we selected this quantity as optimum for all subsequent reactions Furthermore various solvents such as ethanol, methanol and acetonitrile, were investigated and were shown to have a significant impact on the yield of the reaction. The desired product was obtained in fairly good yields with high purity up to 97% when the reaction was carried out with catalyst of BN-PT-SO_3H solid acid and solvent free in MW conditions at 10 min (**Table 1 entries 6**). Moderate yields were observed when either ethanol, methanol, or acetonitrile were used reflux conditions at 24h (Table 1 entries 3-5). The yield decreased and longer reaction time was required to proceed the reaction with ethanol, or methanol, (Table 1 entries 1-2). Consequently, all reactions with BN-PT-SO_3H catalyst was conducted without solvent. Whilst optimising the reaction conditions (Table 1), monitored by TLC, we observed that the use of a solvent needed a longer reaction time whilst the yield of **6a** was lower. Herein we observed that if we conducted the MW 10min reaction at a higher temperature, viz., 140 ˚C some additional spots were observed on the TLC plate thereby suggesting formation of by-products. Also a shorter reaction time showed the presence of starting materials thereby indicating an incomplete reaction. The maximum yield of **6a** (97%) was obtained under a MW condition after heating for 10min.

The re-usability potential of the catalyst BN-Pr-SO_3H was also investigated in the model reaction to synthesise **6a**: briefly, the solid was rinsed with acetonitrile and methanol and heated at 100 ˚C and taken for subsequent reactions. We found that the catalyst could be re-used five times without any significant loss of catalytic activity and concluded that it was sufficient and an important benefit which makes it useful if commercial application is required. The synthesis **(Scheme 2**) of the functionalised ethylpiperazinyl-quinolinyl benzo acridine derivatives **6a-6p** using thecatalyst were undertaken in a MW system for a reaction time of 10 min at 140 ˚C. The yield of the products (**Table 2**) ranged from 75 to 97 %. Compounds **6a-6p** were characterised by IR, ^{1}H NMR, ^{13}C NMR, MS-TOF whilst **6a** included 2DNMR, 90° DEPT and 135° DEPT (the characterisation data are presented in Supporting Information).

To assess the suitability of the MW method, the product was also prepared by a conventional method (thermal method). The physical properties of the product made by the conventional method are shown below:

The yields and total reaction time for synthesised ethylpiperazinyl-quinolinyl acridine derivatives of product 6a, 6b, 6c, 6d, 6e, 6f, 6g, 6h, 6i, 6j, 6k, 6l, 6m, 6n, 6o, and 6p by conventional method were 90, 80, 85, 87, 77, 80, 83, 78, 75, 87, 80, 70, 75, 80, 85 and 65 % for the reaction time 30mins, 1h, 2h, 30mins, 45mins, 30, 30, 1h, 1h, 35mins, 45mins, 30 mins, 1h, 1h, 1h, 1h, respectively. The reaction time was recorded for 10 mins for 6a-6m whilst 6n, 6o, 6p was synthesised in 20 mins. For all these synthesis, 120W was used expect for 6n, 6o, 6p for which 200W MW used.

Table 2. The synthesis of 9-(2-(4-ethylpiperazin-1-yl)quinolin-3-yl)-3,3-dimethyl-3,4,9,10-tetrahydroacridin-1(2H)-one in the presence of BN-PT-SO_3H.

Entry	Substrate (5a-p)	Product (6a-p)	Time (min)	Isolated Yield (%)	M.p. (˚C)
1	$C_6H_5NH_2$	6a	10	97	254-256
2	2-$O_2NC_6H_4NH_2$	6b	10	85	>300
3	4-$O_2NC_6H_4NH_2$	6c	10	90	>300
4	4-$FC_6H_4NH_2$	6d	10	95	275-277
5	4-$ClC_6H_4NH_2$	6e	10	80	>300
6	$Cl_2C_6H_3NH_2$	6f	10	87	290-292
7	4-$BrC_6H_4NH_2$	6g	10	90	270-272
8	o-$CH_3C_6H_4NH_2$	6h	10	87	>300
9	m-$CH_3C_6H_4NH_2$	6i	10	83	>300
10	p-$CH_3C_6H_4NH_2$	6j	10	90	270-272
11	$(CH3)_2C_6H_4NH_2$	6k	10	90	280-282
12	o-C_6H_9NO	6l	10	78	>300
13	p-C_6H_9NO	6m	10	85	>300
14	$C_6H_6N_2$	6n	20	90	>300
15	$C_6H_8N_2$	6o	20	95	>300
16	$C_{10}H_7NH_2$	6p	20	75	>300

2-(4-methylpiperazin-1-yl) quinoline-3-carbaldehyde (1mmol), dimidone (1mmol), and aniline (1mmol), catalyst 0.07g under MW at 140 ˚C.

The IR spectrum of **6a** showed stretching at 3495, and 1681 cm^{-1} for carbonyl and NH groups The ^{1}H NMR spectrum of the compound showed three singlets at δ, 12.98, 8.10, and 4.82 C14-H, C4-H for N19-H, respectively. The C20-CH_2 protons were found at δ, 2.47, d (J = 13.04 Hz) as a doublet and C22-CH_2 δ, 2.47 d, (J = 16.32 Hz,) as a doublet, respectively. ^{13}C NMR spectrum showed the presence of one carbonyl groups at δ 197.17, the structure was further confirmed on the basis of 2D NMR spectral studies.

The selected HMBC correlation of compound 6a is shown in (see **Fig. 1**) The C,H-COSY correlation assigned the carbon signals at δ 26.95, 41, 50.88, 115.01, 122.11, 130.32, 128,98, and 141.10, to C14, C20, C22 , C16 , C15,

C7, C5 and C4 respectively. The carbon signal at δ 141.10, was due to quinolinyl C4-carbon.

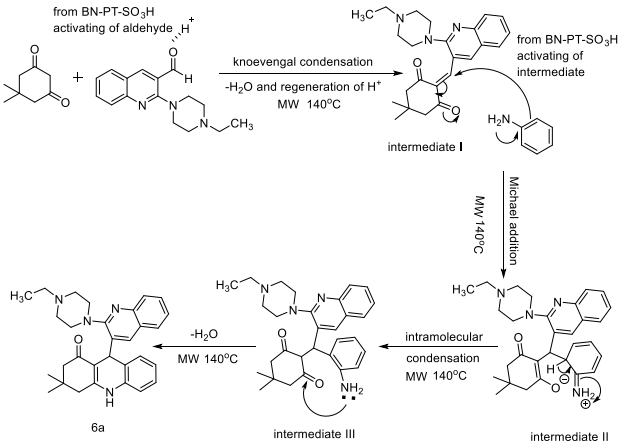

Scheme 3. Proposed mechanism for the synthesis of 9-(2-(4-ethylpiperazin-1-yl)quinolin-3-yl)-3,3-dimethyl-3,4,9,10-tetrahydroacridin-1(2H)-one 6a at MW140 °C.

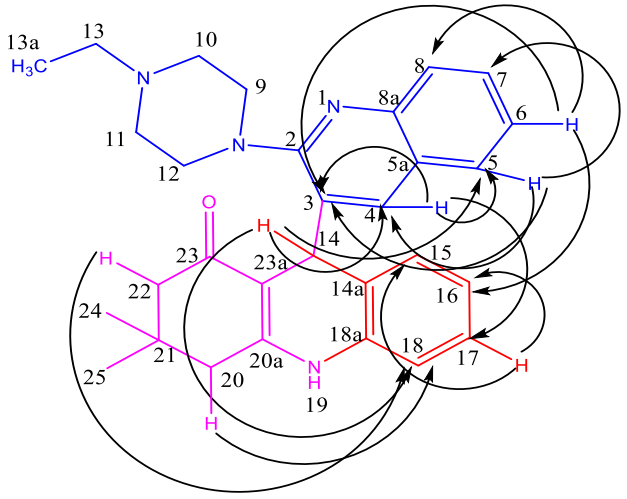

Fig. 1. Selected HMBC correlations of compound 6a.

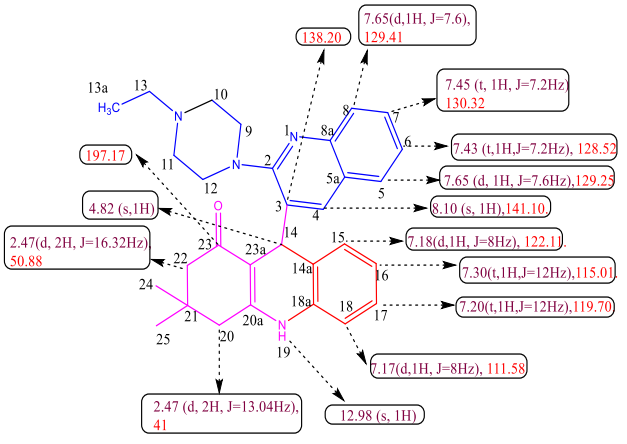

Fig. 2. Selected ^{1}H and ^{13}C NMR and HMBC chemical shifts of 6a.

The H, HCOSY spectrum of the compound revealed the singlet at δ 4.82 which confirmed only one nearby hydrogen to C4 that indicated the compound. The long range HMBC correlation showed the correlation of characteristic C14-H with quinolinyl carbon (C4) at δ 141.10, (C5) at δ 129.25and (C18) δ 111.58 ppm, C4-H with quinolinyl carbon (C5) at δ 129.25, (C3) at δ 138.20, and C17 δ (119.70) ppm respectively. Similarly, C5-H with quinolinyl carbon (C7) at δ 130.32, (C3) at δ 138.20, and C4 δ (142.96) ppm, C6-H with quinolinyl carbon (C8) at δ 129.41, (C3) at δ 138.20, and C16 at δ (115.01) ppm, C17-H with quinolinyl carbon (C16) at δ 115.01, (C15) at δ 122.11 ppm, C20-H with quinolinyl carbon (C18) at δ 111.58, ppm, C22-H with quinolinyl carbon (C18) at δ 111.58,ppm, respectively. Based on the above spectral details and its elemental analysis, the structure was confirmed as of 9-(2-(4-ethylpiperazin-1-yl)quinolin-3-yl)-3,3-dimethyl-3,4,9,10-tetrahydroacridin-1(2H)-one 6a and Selected ^{1}H and ^{13}C NMR and HMBC chemical shifts of 6a (see **Fig. 2**)Thus the one pot multi-component synthesis of the new ethylpiperazinyl-quinolinyl acridine derivatives using the less studied BN-PT-SO_3H is a neat and efficient reaction which is selective for the formation of the sought after target.

A proposed mechanism (Scheme 3) is presented to support the formation of **6a** which was the model reaction for the new reaction scheme. In the first step, the acidic catalyst activates the aldehyde carbonyl functionality thereby enabling dimidone to form a new covalent bond with loss of water as in the Knoevenagel condensation to produce 5, 5-dimethyl-2-((2-(4-ethylpiperazin-1-yl)quinolin-3-yl) methylene) cyclohexane-1,3-dione as an intermediate**I**. In the next step, the catalyst activates the intermediate **I** thereby facilitating a Michael addition to give intermediate **II**. This is followed by a simple intramolecular condensation reaction to produce intermediate **III** which subsequently undergoes a proton transfer reaction to produce **6a**.

Computational docking results

Molecular docking is a computational technique that samples conformations of small compounds in protein binding sites; scoring functions are used to assess which of these conformations are best complements to the protein binding site. There are two main aspects to assess the quality of docking methods: (i) docking accuracy, which recognizes the true binding mode of the ligands to the target protein and (ii) screening enrichment which measures the relative improvement in the identification of true binding ligands using a docking method versus random screening [**36**].

A training set of 16 compounds as well as 1150 (74 may bridge and 1076 Scaffold) hit compounds retrieved from the databases which satisfied drug-like properties were docked in the active site of Hsp90 using Ligand Fit programme. In order to support the experimental results, computational docking analysis was performed to create a model for Hsp90 (heat shock protein 90) –compound **6a & 6d** complex. It had been stated earlier, that each domain of the SA proteins contains two sub domains (IA and B, IIA and B, IIIA and B); that they possess common structural

motifs. Sudlow site I and Sudlow site II (subdomains IIA and IIIA respectively) are the most probable binding sites of the ligands. Molecular docking analysis was performed using Auto dock 4.2 program and the energetically most feasible Hsp90-compound **6a & 6d** complex are displayed in **Fig. 3 (a-b).**

Docking results clearly point out that compound **6a & 6d** bind inside the binding pocket located in subdomain II A of Hsp90. It can be seen from **Fig. 3** (**a-b**), compounds **6a & 6d** are located adjacent to the amino acid residues were mapped on ASP93 and LYS58 residues. The 6a&6d compounds show hydrogen bond and hydrophobic interactions with ASP93, ASN51, ALA55, LYS58, GLU97, MET98, and SER-99, respectively. **Fig. 3(a, b)** represents the binding orientation of the hit compounds and also shows how well the compounds fit into hydrogen bonding. The compounds were further sorted; based on the consensus scoring function. The training set compounds showed the dock score greater than 80 and the maximum fit value of 10. All of the hit compounds possessed the maximum fit value of 11 and the dock score of more than 85. Some of the active compounds in the training set show hydrogen bonding and hydrophobic interaction with the two active site residues of ASP93, LYS58 and with few hydrophobic residues (ASN51, ALA55, LYS58, MET98, and SER-99) were considered to be crucial for inhibitory activity.

The hit compounds showed very good interactions with the critical residues of ASP93 and LYS58. It is imperative to note from the computational observations that compound **6a & 6d** are in the locality of LYS58 amino acid residue of Hsp90. The obtained values just provide the probable geometry of the complexes; however the binding has been established experimentally. The ability of Hsp90 to clamp onto proteins allows amino acid residues to perform several functions including assisting folding, preventing aggregation, and facilitating transport.

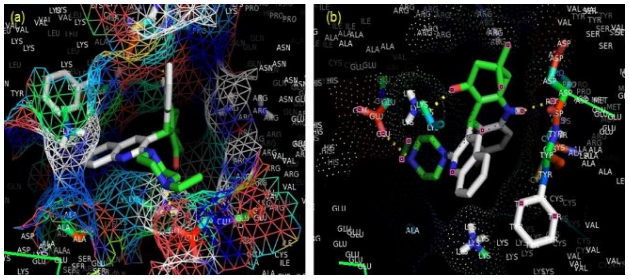

Fig. 3. (a) Molecular docking of the Hsp90-compound **6a** and (b) Hsp90-compound **6d** complex selected amino acid residues are represented by stick and cartoon models. Hydrogen bond is shown in yellow dotted line.

Conclusion

The preparation of the catalyst is simple and safe whilst demonstrating only 10 % loss in catalytic activity after five cycles of re-use thereby making it cost-effective for possible industrial application. The synthesised acid catalyst was subsequently used in a new one pot reaction for the synthesis of highly functionalised ethylpiperazinyl-quinolinyl acridinone derivatives. This reaction under MW conditions is relatively very fast, safe, and environmentally friendly and gives high yields. Furthermore, the one pot reaction used in this study gives rise to new types of ethylpiperazinyl-quinolinyl acridine derivatives which have suitable functionalities for a host of possible biological applications such as Hsp90 protein binding molecular docking studies.

Acknowledgements

The authors gratefully acknowledge the financial support of the National Research Foundation (NRF) and Durban University of Technology (DUT).

References

1. (a) Dömling, A.; *Chem. Rev.* **2006,** *106*, 17. **DOI:** 10.1021/cr0505728
(b) Zhu, J.; *Eur. J. Org. Chem.* **2003**, 1133. **DOI:** 10.1002/ejoc.200390167
(c) Dömling, A.; I.Ugi, I. Angew. *Chem. Int. Ed.* **2000,** *39*, 3168. **DOI:** 10.1002/1521-3773(20000915)39:18<3168:AID-ANIE3168>3.0.CO; 2-U
2. Antonini, I.; Polucci, P.; Kelland, L. R.; Menta, E.; Pescalli, N.; Martelli, S. *J. Med.Chem.* **1999,** *42*, 2535. **DOI:** 10.1021/jm9805586
3. McCarthy, P. J.; Pitts, T. P.; Gunawardana, G. P.; Kelly-Borges, M.; Pomponi, S. A. *J. Nat. Prod* **1992**, *55*, 1664. **DOI:** 10.1021/np50089a016
4. Spalding, D. P.; Chapin, E. C.; Mosher, H. S. *J. Org. Chem.* **1954**, *19*, 357. **DOI:** 10.1021/jo01368a011
5. Demeunynck, M.; Charmantray, F.; Martelli, A. *Curr. Pharm. Des.* **2001**, *7*, 1703. **DOI:** 10.2174/1381612013397131
6. Salimon, J.; Salih, N.; Yousif, E.; Hameed, A.; Kreem, A. *Arab.J. Chem.*, **2010**, *3*, 205. **DOI:** 10.1016/j.arabjc.2010.06.001
7. Saercey, M.; Martin, P.N.; Howarth, N.M.; Madden, B.; Wakelin, L.P.G. *Bioorg. Med. Chem. Lett.* **1996**, *6*, 1831. **DOI:** 10.1016/0960-894X (96)00325-3
8. Filloux, N.; Galy, J. P. *Synlett* **2001,** 1137. **DOI:** 10.1055/s-2001-15137
9. Antonini, I.; Polucci, P.; Magnano, A.; Cacciamani, D.; Konieczny, M. T.; Paradziej-Łukowicz, J.; Martelli, S. *Bioorg. Med. Chem.* **2003,** *11*, 399. **DOI:** 10.1016/S0968-0896(02)00442-X
10. Szakacs, G.; Paterson, J.K.; Ludwig, J.A.; Booth-Genthe, C.; Gottesman, M.M. *Nat.Rev. Drug Discov.* **2006**, *5*, 219. **DOI:** 10.1038/nrd1984
11. Bach, P.B.; Jett, J.R.; Pastorino, U.; Tockman, M.S.; Swensen, S.J.; Begg, C.B. *JAMA.*, **2007**, *297*, 953. **DOI:** 10.1001/jama.297.9.953.
12. Chen, J.; Wang, Z.; Li, C.M.; Lu, Y.; Vaddady, P.K.; Meibohm, B.;Dalton, J.T.; Miller, D. D.; Li, W. *J. Med. Chem.*, **2010,** *53*, 7414. **DOI:** 10.1021/jm100884b
13. O'Connor, R. *Curr. Cancer Drug Targ.* **2009**, *9*, 273. **DOI:** 10.2174/156800909788166583
14. Shavit, Y.; Ben-Eliyahu, S.; Zeidel, A.; Beilin, B. *Neuroimmunomodulation*, **2004,** *11*, 255. **DOI:** 10.1159/000078444
15. Arve, L.; Voigt, T.; Waldmann, H. *QSAR Comb. Sci.*, **2006,** *25*, 449. **DOI:** 10.1002/qsar.200540213
16. Li, Y.; Xu, X.; Shi, D.; Ji, S. *Chin. J. Chem.* **2009**, *27*, 1510. **DOI:** 10.1002/cjoc.200990254
17. Jin, J.; Zhang, J.; Liu, F.; Shang, W.; Xin, Y.; Zhu, S. *Chin. J.Chem.* **2010,** *28*, 1217. **DOI:**10.1002/cjoc.201090211
18. Nadaraj, V.; Thamarai Selvi, S.; Mohan, S. *Eur. J. Med. Chem.* **2009**, *44*, 976. **DOI:**10.1016/j.ejmech.2008.07.004

19. Tu, S.; Jia, R.; Jiang, B.; Zhang, Y.; Zhang, J. *J. Heterocycl. Chem.* **2006,** *43*, 1621. **DOI:**10.1002/jhet.5570430629
20. Zang, H.; Zhang, Y.; Zang, Y.; Cheng, B. W. *Ultrason. Sonochem.* **2010,** *17*, 495. **DOI:**10.1016/j.ultsonch.2009.11.003
21. Bahrami, K.; Khodaei, M. M.; Fattahpour, P. *Catal. Sci. Technol*. **2011**, *1*, 389. **DOI:** 10.1039/c1cy00053e
22. Van Rhijn, W. M.; De Vos, D. E.; Sels, B. F.; Bossaert, W. D.; Jacobs, P. A. *Chem. Commun*. **1998**, 317. **DOI:** 10.1039/A707462J
23. Karimi, B.; Zareyee, D. *Org. Lett.* **2008**, *10*, 3989. **DOI:** 10.1021/ol8013107
24. Kureshy, R. I.; Ahmad, I.; Pathak, K.; Khan, N. H.; Abdi, S. H.R.; Jasra, R. V. *Catal. Commun.* **2009**, *10*, 572. **DOI:** 10.1016/j.catcom.2008.10.035
25. Das, B.; Venkateswarlu, K.; Holla, H.; Krishnaiah, M. *J. Mol.Catal. A: Chem.* **2006,** *253*, 107. **DOI:** 10.1016/j.molcata.2006.03.011
26. Van Rhijn, w. M.; De Vos, D. E.; Sels, B. F.; Bossaert, W. D.; Jacobs, P. A. Chem. Commun. **1998**, 317. **DOI:** 10.1039/A707462J
27. Karimi, B. Zareyee, D. Org. Lett. **2008**, *10*, 3989. **DOI:** 10.1021/ol8013107
28. Kureshy, R.I.; Ahmad, I. Pathak, K. Khan, N.H.; Abdi, S.H.R.; Jasra, R. V. Catal. Commun. **2009**, *10*, 572. **DOI:** 10.1016/j.catcom.2008.10.035
29. Das, B. Venkateswarlu, K. Holla, H. Krishnaiah, M. J. Mol. Catal. A: Chem. **2006,** *253*, 107. **DOI:** 10.1016/j.molcata.2006.03.011
30. Valentini, L. Macan, J. Armentano, I. Mengoni, F. Kenny, J.M. Carbon. **2006**, *44*, 2196. **DOI:**10.1016/j.carbon.2006.03.007
31. Kathi, J. Rhee, K.Y. J. Mater. Sci. **2008**, *43*, 33. **DOI:** 10.1007/s10853-007-2209-2
32. Gianni, C. Giada, G. Genchi.; Ioannis, L. Athanassia, A. Dinuccio, D.Federica, C. Virgilio, M. Journal of Colloid and Interface Science. **2012**, *374*, 308. **DOI:** 10.1016/j.jcis.2012.01.049
33. Dutta, A. K.; Gogoi, P. Borah, R. *RSC Adv.* **2014**, *4*, 41287. **DOI:** 10.1039/C4RA07323A
34. Cohn, O. M.; Narine, B.; Tarnowski, B. *J. Chem Soc. Perkin Trans.* **1981**, *1*, 1520. **DOI:** 10.1039/P19810001520
35. Sakkiah, S. Thangapandian, S. John, S. Kwon Y. J.; Lee K.W. European Journal of Medicinal Chemistry. **2010,** *45*, 2132. **DOI:** 10.1016/j.ejmech.2010.01.016
36. Muthas, D. Yogesh, A. S.; Lundborg, M. Karlen, A. *J. Mol. Graph. Model.* **2008,** *26*, 1237. **DOI:**10.1016/j.jmgm.2007.11.005

Supporting Information

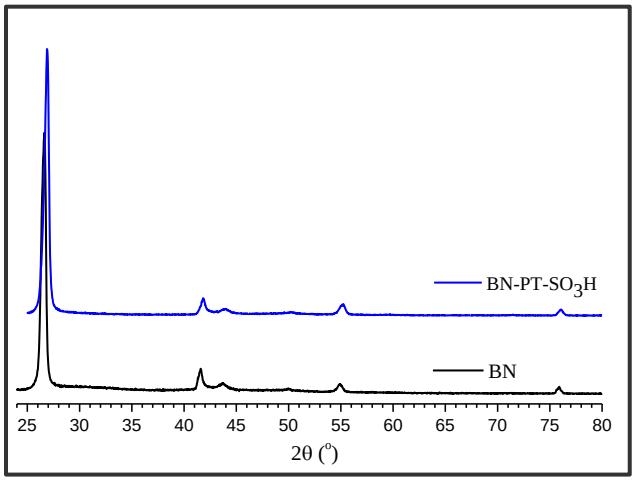

Fig. S1. PXRD pattern of BN and BN-PT-SO_3H.

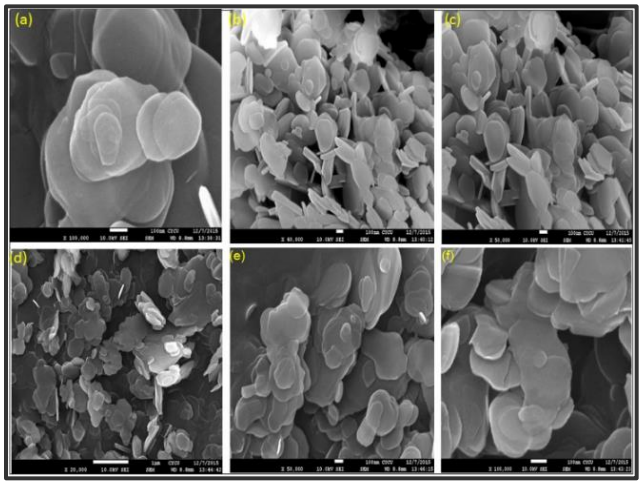

Fig. S2. SEM image of BN (a, b and c) and BN-PT-SO_3H (d, e and f).

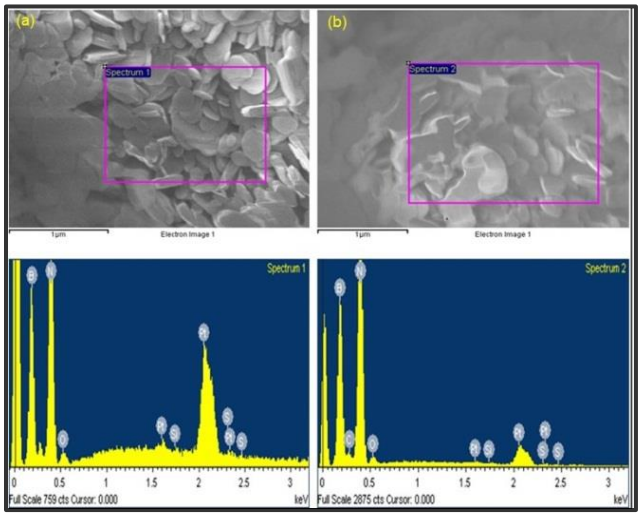

Fig. S3. EDS pattern for BN (image a) and BN-PT-SO_3H (image b).

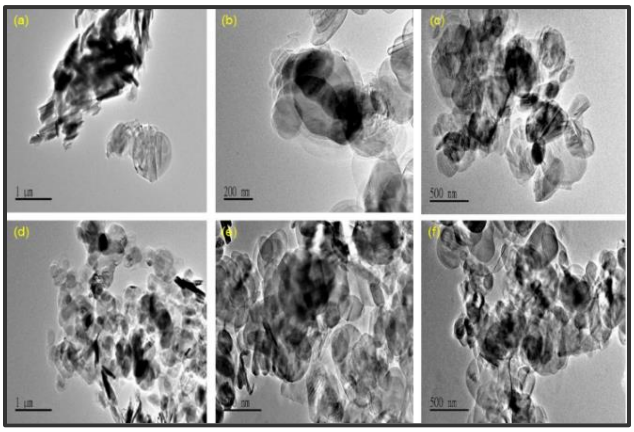

Fig. S4. TEM image of BN (a, b and c) and BN-PT-SO_3H (d, e and f).)

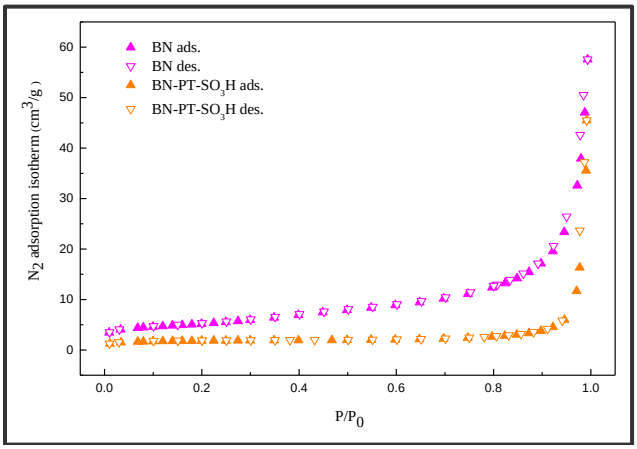

Fig. S5. Adsorption and desorption isotherms of BN and BN-PT-SO_3H at 273K.

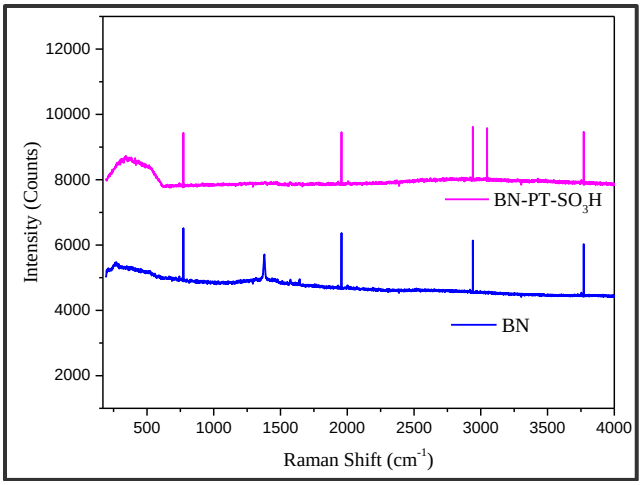

Fig. S6. Raman Shift of BN and BN-PT-SO_3H.

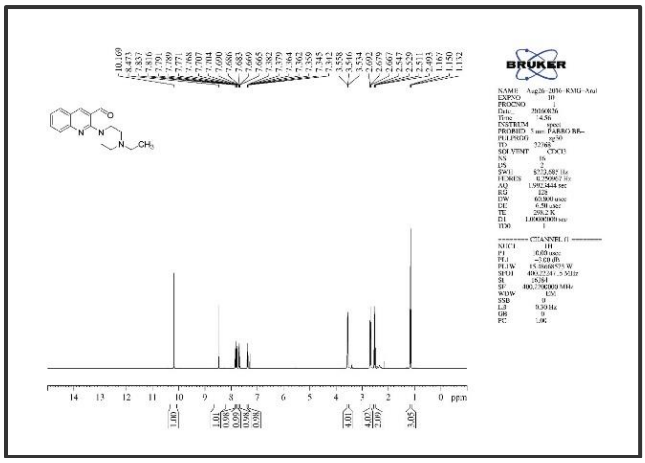

Fig. S7. The ^{1}H NMR of compound 3

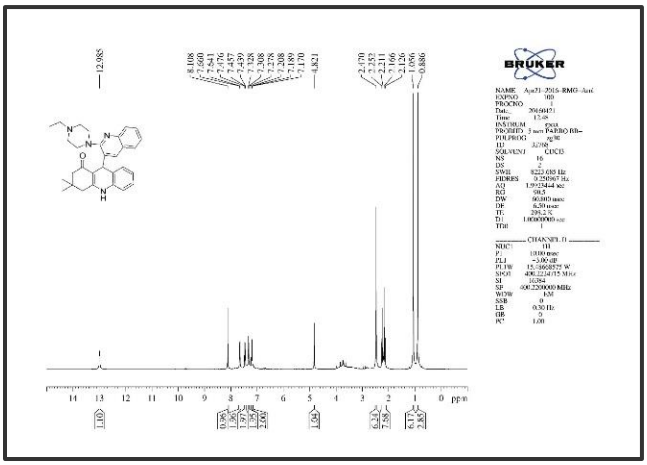

Fig. S9. The ^{1}H NMR of compound 6a

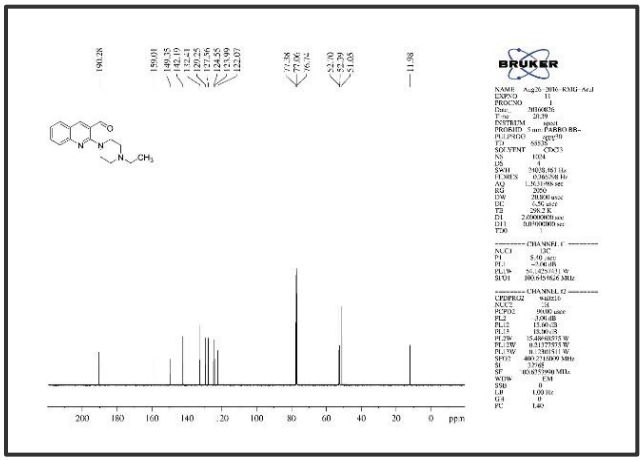

Fig. S8. The ^{13}C NMR of compound 3.

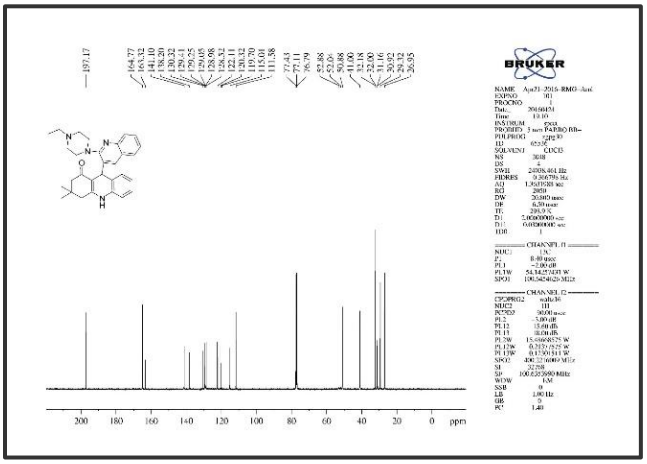

Fig. S10. The ^{13}C NMR of compound 6a